Chinese Chemical Letters 31 (2020) 1060–1070

Contents lists available at ScienceDirect

Chinese Chemical Letters

journal homepage: www.elsevier.com/locate/cclet

Review

Metal-organic framework-based nanomaterials for biomedical applications

Shu Zhang[a,b], Xibo Pei[a,b], Huile Gao[c], Song Chen[a,b], Jian Wang[a,b,*]

[a] State Key Laboratory of Oral Diseases, National Clinical Research Center for Oral Diseases, West China Hospital of Stomatology, Sichuan University, Chengdu 610041, China
[b] West China School of Stomatology, Sichuan University, Chengdu 610041, China
[c] Key Laboratory of Drug Targeting and Drug Delivery Systems, West China School of Pharmacy, Sichuan University, Chengdu 610041, China

ARTICLE INFO

Article history:
Received 19 September 2019
Received in revised form 19 November 2019
Accepted 20 November 2019
Available online 21 November 2019

Keywords:
Nanoscale metal-organic framework (nMOF)
Biomaterial
Functionalization
Biological applications
Nanocarrier

ABSTRACT

In the past decade, nanoscale metal-organic frameworks (nMOFs) have drawn a great attention due to their high porosity, wide range of pore shapes, tunable frameworks and relatively low toxic. With the development of nanotechnology, many researchers studied the synthesis, characterization, functionalization and biotoxicity of nMOFs, and a more thorough understanding was developed about numerous nMOFs as promising platforms for biomedical applications. This review highlights the up-to-date progress of nMOFs related to their bio-applications such as drug delivery, bioimaging, biosensing and biocatalysis, and the common surface modification methods were classified into four categories: covalent post-synthetically modification, coordinative post-synthetically modification, noncovalent post-synthetically modification and modification on the external surface. At the same time, the challenges and perspectives of nMOFs were discussed as well.

1. Introduction

Metal-organic frameworks (MOFs), also known as coordination polymers or porous coordination networks, were first reported in 1989 [1]. These hybrid inorganic-organic solids can be easily tuned due to the extended network structures formed by the self-assembly of metal-connecting nodes and multitopic organic linkers [2]. The flexible combination of metal inorganic centers and organic ligands enable diverse designs of MOFs with high porosity structures, which makes them different from other nanoparticles. As an emerging and promising class of porous hybrid materials, these materials have drawn great attention for various applications because of their unique features, including high porosity, wide range of pore shapes, large surface area and tunable frameworks. During the past two decades, a number of potential applications related to MOFs have been reported such as gas storage and separation [3–11], catalysis [12–19], sensing [20,21], magnetism [22] and energy [23–25]. On the other hand, MOFs were studied on potential biomedical applications, including biological sensing [26,27], optical molecular imaging [28–31] and drug delivery [28–30,32–36].

Recently, with the development of nanotechnology, MOFs have been reduced down to nanoscale particles metal-organic frameworks (nMOFs). As expected, the nMOFs possess not only the properties of porous materials but nanometer scale size as well, thus their fascinating property leads to a great superiority in biomedicine field [37]. Since Ferey and co-workers first published the loading and release of the drugs encapsulated into MOFs in 2006 [38], numerous studies have been reported related to the post-synthetic modification of nMOFs and the incorporation of multiple functional groups, such as biological molecules and small-molecule fluorescent materials. Compared to former nanocarriers (inorganic zeolites, gold, silica nanoparticles and others), nMOFs exhibit four major advantages for biomedical applications. Firstly, nMOFs can be designed into desired structures, allowing the load of various functional materials with different shapes and sizes. Secondly, the high porosity and large surface area contribute to their drug delivery properties such as high loading capacity and efficient transport of biomolecules/drugs [39,40]. Thirdly, nMOFs are biodegradable as a result of weak coordination bonds, which is essential for controllable release of the drugs. Finally, multifunctional nMOFs exhibit the ability of targeting cancer cell in a highly selective manner. As a result, these excellent properties bring nMOFs to a promising stage for biomedical applications.

* Corresponding author at: State Key Laboratory of Oral Diseases, National Clinical Research Center for Oral Diseases, West China Hospital of Stomatology, Sichuan University, Chengdu 610041, China
E-mail address: ferowang@hotmail.com (J. Wang).

https://doi.org/10.1016/j.cclet.2019.11.036
1001-8417/

Although MOFs have earned more and more attention and many works have been done in recent studies, the applications of nMOFs in biomedical field are still at an outset stage [41–45]. In this review, we will summarize various functionalization methods of nMOFs and focus on the progress related to their bio-applications so far. We will first review all the approaches commonly used to modify nMOFs in biomedicine aspects and highlight the developments of nMOFs in biomedical fields such as drug delivery, controllable release carrier, biological sensing, optical molecular imaging, cancer therapy and so on. Finally, challenges of the nMOFs will be discussed, as well as the prospects for the future biological applications. Unlike the former remarkable reviews, this review not only discusses the all-around bio-applications of nMOFs, but gives an eye to their toxicity evaluation *in vivo* as well. This article is designed to provide new directions for nMOFs' future research and give an outlook on the potential clinical applications.

2. Surface modification of MOF nanoparticles

So far, a large number of nanomaterials have been applied to biomedical fields, such as nanoemulsions [46], lipid/polymer-based nanoformulae and nanoparticles [47–49]. In order to facilitate the delivery of bioactive molecules and reduce the side effects, strategies have been performed to modify nMOFs for various biomedical applications. Surface modifications are common approaches for functionalization of nMOFs, which overcome several challenges related to the stability and/or the targeting abilities [50]. The surface modifications are generally divided into four categories. (i) Covalent post-synthetically modification. In this type of modification, the drugs/biomolecules are usually conjugated with MOF linker, such as click chemistry and conjugation reactions. (ii) Coordination modulation and coordinative post-synthetically modification. The drugs/biomolecules are coordinated to the metal clusters of the MOFs *via* coordination chemistry such as ligand exchange. (iii) Non-covalent post-synthetically modification, including electrostatic interactions, hydrogen bonding and dispersion forces. (iv) Modifications on the external surfaces of MOFs, usually performed conjugating the drugs/biomolecules to the silica coating on the MOFs. In this section, we will summarize the different modification methods and discuss the individual advantage and deficiencies of these strategies.

2.1. Covalent post-synthetically modification

The drugs and biomolecules can attach to the linkers and frameworks in the MOFs through covalent coupling. Kiang and coworkers first reported the successful covalent post-synthetic modification in 1999 [51]. Since then numerous researchers have studied the covalent post-synthetic modifications. Canivet *et al.* reported the peptides conjugation to free amine groups on the linker of (In) MIL-68-NH_2 MOFs, and the structures of the MOFs remained steady during modification process [52]. As for biomacromolecules such as nucleic acid and proteins, coordinative post-synthetically modification is still a promising method. Morris *et al.* first published the test of DNA conjugation to MOF structures *via* click chemistry [53]. Kahn *et al.* reported a new stimuli-responsive DNA-MOF system *via* EDC/NHS amide coupling reaction between amine-modified cytosine-rich DNA and carboxylic acid-functionalized MOFs [54]. In addition, the proteins' nucleophiles such as amines, hydroxyls and thiols enable these proteins to conjugate to MOF linkers covalently by nucleophilic substitutions. Lin *et al.* reported the attachment of the amine groups in trypsin to the unmodified carboxylate groups in MOFs *via* nucleophilic substitution [55]. Jung *et al.* established the conjugation of green fluorescent protein (EGFP) with MOFs through DCC or EDC coupling [56]. However, the presence of electrophiles in MOFs might be the key for covalent conjugation of proteins.

2.2. Coordination modification

Coordination modification is commonly used to modify MOFs for biomedical applications, which can occur during the synthetic process or post synthesis. Surface modification of MOFs performed during the synthetic process is based on coordination modulation, with carboxylate-containing molecule serving as a modulator. Abánades Lázaro *et al.* recently introduced the biomolecules biotin and folic acid on the surfaces of UiO-66 by coordination modulation during the synthetic process [57]. In this case, the folic acid molecules were utilized as the MOF linkers and surface ligands (Fig. 1). Dong *et al.* prepared TCCP@UiO-66 with the porphyrin on the surface through a similar strategy, and the obtained MOFs exhibited a good porous property [59]. On the other hand, nucleophilic functional groups including phosphates, thiols, carboxylates, and imidazoles can be used to modify the surface of MOFs post-synthetically *via* coordination of moieties to metal

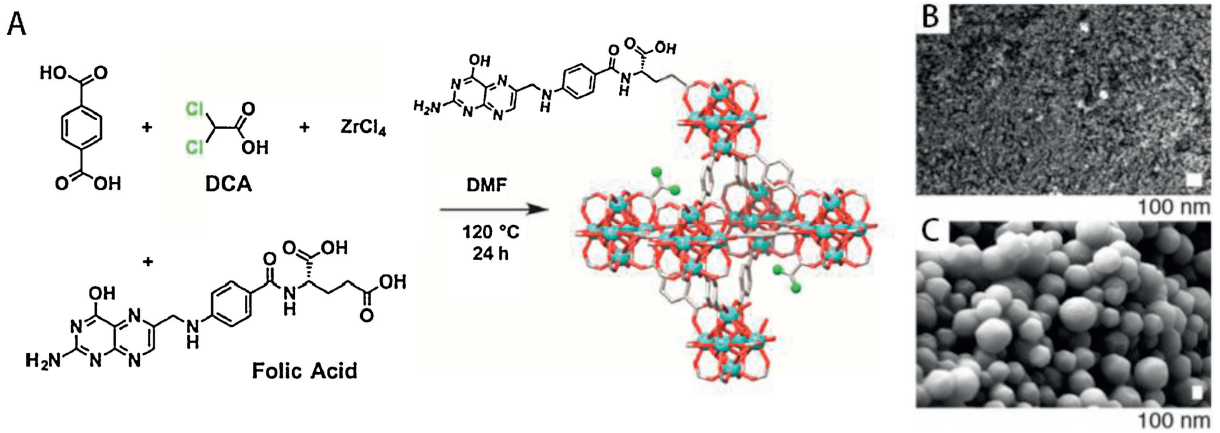

Fig. 1. "Click modulation" surface functionalization protocol for UiO-66. (A) Schematic synthesis of UiO-66 modulated by dichloroacetic acid and folic acid, showing incorporation of both modulators at defect and surface sites. (B) SEM images of UiO-66-FA. (C) SEM images of UiO-66-L2-PNIPAM, showing a rounded morphology due to the polymer coating. Reproduced with permission [57]. Copyright 2018, American Chemical Society.

cluster nodes [58–63]. These biomolecules perhaps coordinate to unsaturated metal cluster nodes or replace linkers on the surface, which was also called surface ligand exchange. For example, Wang *et al.* reported the post-synthetic incorporation of carboxyl-functionalized diiodo-substituted BODIPY onto the UiO-66 surfaces [62]. Lin and coworkers attached the small interfering RNA (siRNA) to the Zr^{4+} present on the surface of UiO-68-NH_2 through the phosphate groups of siRNA [63].

2.3. Noncovalent post-synthetically modification

Some biomacromolecule can be attached to the surface of MOFs through controlled supramolecular interactions. Hong *et al.* synthesized a radiolabeled model of UiO-66 [64]. The MOFs were functionalized with pyrene-derived PEG *via* π-π stacking interactions, and then the terminal maleimide residue in pyrene-derived PEG chains reacted with the cysteine residues in nucleolin-targeting peptide post-synthetically. Ma *et al.* formed a novel protein-coated MOF system to monitor real-time glucose change [65]. Glucose dehydrogenase (GDH) and methylene green (MG) were adsorbed onto the external surface of ZIFs through several strong interactions between the biomacromolecules and ZIFs. This type of modification gives a promising method for the functionalization of bulky molecules.

2.4. External modification

Biomolecules can also be modified on the external surface of MOF nanoparticles. In this type of modification, an outside silica coating is required as a platform to attach extra drugs or biomolecules to the surface of MOFs. Yang *et al.* and Taylor *et al.* successfully grafted the silyl derived cyclic oligopeptide c(RGDfK) onto the surface of Fc-Gd and MIL-101 MOF nanoparticles with a silica coating for tumor-targeting, respectively [29,66]. Zhang *et al.* also reported their studies on attaching SGDEVDK oligopeptide onto the surface of nMOFs *via* a silica coating [67]. Huang *et al.* presented another example of the coupling between folic acid and the silica coating on Fe(bbi) MOFs [68]. But the new toxicity caused by exogenous silica is still a challenge for the application of this silica-coating method.

As the rapid development of nanotechnology, there are great deal of studies on decorating the MOF nanoparticles for biological applications, both during the synthetic process and post synthesis. Despite the particular innovation and advantage of these methods, the restriction and applicability should be considered as well, such as stability, efficiency, biocompatibility and synthetic inconveniences. And a comprehensive comparison of several modified approaches is also needed in the future work.

3. Biomedical applications of nMOFs

Because of the unique properties including large surface area, high porosity, nanometer scale and biodegradability, more and more reports believe that the nMOFs have the potential for biomedical applications. For drug delivery, the appropriate design or formulation of these nanocarriers can effectively change the hydrophilicity of the drugs, achieve the controlled delivery, prevent drugs nonspecifically binding to irrelevant molecules, and influence the uptake and excretion of the drugs [69–72]. For biological sensing, the large specific surface area and wide range of pore shapes allow various conjugation methods for designing biosensors, which enable the specific molecular recognition [73–76]. For imaging, the nMOFs can be modified with imaging contrast agents and develop promising targeted platforms for optical molecular imaging, magnetic resonance imaging (MRI) and X-ray computed tomography imaging (CT) [77,78]. However, as a type of material used for biological applications especially for *in vivo* clinical applications, many requirements related to their toxicity, biodistribution and chemical stability should be considered thoroughly. In recent studies, great progress has been made and works on these strict demands have been progressively investigated. The synthesis strategies and functionalization methods of nMOFs have rapidly advanced and enabled various biomedical applications. In the following section, we will present an overview on the different biological applications of nMOFs and discuss their relevant bio-safety *in vitro* and *in vivo*.

3.1. Drug delivery

3.1.1. Encapsulation of the drug molecules

Due to the high porosity and tunable structure of nMOFs, noncovalent encapsulation has become the most common way to incorporate drug molecules into nMOFs. The encapsulation routes include two-step encapsulation and in-situ encapsulation routes. The two-step encapsulation route is a method to load molecules through immersing the nMOFs in the specific solution. The nMOF pores allow suitable accommodation for molecules if their sizes are smaller than those pores, and molecules are encapsulated successfully by the noncovalent bonding between the molecules and the nMOFs. For example, Horcajada *et al.* formed a series nMOFs with the encapsulation of hydrophobic molecules by noncovalent interaction [30,38]. Besides the drug molecules, other small biological molecules like oligopeptide and oligonucleotides molecules can also be encapsulated into the pores of nMOF *via* diffusion [79–84]. This kind of encapsulation does not involve any additional reactions to incorporate the biological molecules, but the sizes of these biological molecules must be small enough to diffuse into the pores of nMOFs.

On the other hand, if the sizes of molecules are larger than the pores in the nMOFs, *in-situ* encapsulation can be a good choice to encapsulate these large molecules into nMOFs. For example, proteins, the biological macromolecules, unlike those small size molecules, the bulky structures make it difficult to be encapsulated into MOFs directly. Proteins are dispersed in the solution where MOFs are been synthesized and then the MOF particles are formed around proteins. As a result, the proteins are encapsulated into MOFs eventually [85–87]. In addition, more and more works have been done on using MOFs for the de novo encapsulations of bulky biological macromolecules [88–90]. The strong coordination interactions, hydrophobic interactions and intermolecular hydrogen bonding between the proteins and metal cluster nodes are the basis of successful encapsulation.

3.1.2. X-based nMOF nanocarriers (X = Cr, Fe, Cu, Gd, Zr)

Férey *et al.* first suggested the potential of MOFs in the field of drug delivery in 2006 [38]. They formed MIL-100(Cr) and MIL-101(Cr) with remarkable IBU loading capacities and the subsequent studies showed that the IBU was progressively released in simulated body fluid. This report established a new MOF-based drug delivery system, which exhibited both higher drug-loading capacity and controlled-release property. But regarding the toxicity of Cr compounds, some MOFs with low toxicity and biodegradability are considered more suitable for incorporating and delivering the drug molecules. For instance, Fe-based, Cu-based and Gd-based MOFs exhibited a lower loading capacity and longer time for the full release of the incorporated drug due to the smaller pore size of this material [30,32,53,63,91–93]. Kundu *et al.* first reported the investigation concerning the biodistribution and toxicology parameters of the drug-loaded nMOFs *in vivo* [91]. In this work, they presented a Gd-based MOF (Gd-pDBI) with the incorporation of doxorubicin (DOX) molecules. The DOX loaded Gd-pDBI mainly accumulated in the liver and exhibited both the

excellent biocompatibility and significant anticancer activity *in vivo*.

3.1.3. Zr-based MOFs nanocarriers

Recently, drug delivery systems based on Zr-based MOFs have aroused an increasing interest because of the excellent biocompatibility of zirconium [61–64,94,95]. Hong *et al.* formed several drug-loaded nMOFs and investigated their distribution and clearance in nude mice [64]. No untoward effect or evident toxicity was found in the experimental animals treated with different doses of UiO-66-Py-PGA-PEG for 30 days. At 2 h post-injection, a high accumulation appeared in the liver and spleen while no radioactivity was found in the bone or kidney. Lin and coworkers represented another new nanocarrier platform UiO nMOF for the co-delivery of cisplatin prodrug and siRNAs [63]. This unique nMOF platform exhibited an enhancement in chemotherapeutic efficacy *in vitro* (Fig. 2), but the biosafety evaluation was not mentioned.

In addition, unlike the pH-responsive or temperature-responsive controlled-release systems, Hill *et al.* published a rather novel light-triggered drug delivery system [94]. A thin UiO-66 MOF was coated on the optical fiber, and then 5-FU was encapsulated into the MOFs. The release of loaded drug was triggered by light at 1050 nm. This study showed a different strategy for light-triggered drug release.

3.1.4. ZIF-8 nanocarriers

Other porous nMOFs like Zinc-based nMOFs have attracted a raising attention in the drug delivery aspect due to the hypotoxicity of Zn^{2+} and relatively large pore cavities. Among this kind of materials, zeolitic imidazole framework (ZIF-8), consisted of zinc ions and 2-methylimidazolate, provides a new method to deliver the drug molecules. Yaghi and co-workers first formed ZIF-8 in 2006 and the excellent performance prompted the applications related to drug delivery [96]. Sun *et al.* first reported the incorporation of drug molecules with ZIF-8 [97]. They loaded 5-Fu into ZIF-8 and then observed the release process of the drug. During the early stage, 50% of the drug was released from ZIF-8 and the stable release continued 7 days in PBS. Meanwhile, the 5-Fu exhibited a more rapid releasing in acetate buffer because of the decomposition of ZIF-8, which enabled the establishment of a pH-responsive controlled-release system. Since then, a number of researches have been carried out to study ZIF-8 for drug delivery *in vitro* and *in vivo* (Fig. 3) [98–101]. For instance, Wang *et al.* loaded the anticancer drug DOX into ZIF-8 nanoparticles and studied its toxicity and antitumor efficacy *via* tumor-bearing mice model [98]. *In vitro* and *in vivo* experiments demonstrated that the DOX-loaded ZIF-8 was biocompatible and obviously antineoplastic, which making it a potential nanocarrier for cancer theranostics.

Most recently, a novel dimethyloxalylglycine(DMOG) loaded-ZIF-8-coated implant was reported by Wang and coworkers [102]. They successfully introduced the DMOG into ZIF-8-coated titanium implant without influencing the morphology and degradation of ZIF-8 coating. *In vitro* tests showed that the formed complex exhibited a significant enhancement of osteogenic and angiogenic activity as well as excellent biocompatibility, which allow it to be a promising strategy for implant modification.

Despite the hypotoxicity of ZIF-8, the toxicity caused by the synergistic effect of drugs and ZIF-8 nanoparticles should also be taken into consideration. Chen and co-workers reported the incorporation of 3-methyladenine (3-MA) into ZIF-8 by one-pot synthesis [100]. The loading of 3-MA was calculated as 19.8 wt% and the release of 3-MA from ZIF-8 nanoparticles exhibited to be pH-responsive controlled. *In vitro* tests revealed that a significant toxic effect occurred to the HeLa cells, and biodistribution study showed that zinc mainly accumulated in liver, spleen and lung. The experiments *in vivo* indicated that 3-MA@ZIF-8 had low hepatoxicity and nephrotoxicity, but an obvious antitumor efficacy was also observed.

3.1.5. Bio-MOFs nanocarriers

In recent years, another hopeful nMOF has become more and more popular in drug delivery. Rosi *et al.* published metal-nucleobase syntheses and the obtained products were called "bio-MOFs" [103,104]. The nucleobases were used as organic linkers to coordinate to metal ion clusters through carboxylate chelation and could interact with framework materials. Because of the existence of nucleobases, bio-MOFs exhibit an anionic zeta-potential, which contribute to the succeeding drug loading. An *et al.* first encapsulated the cationic drug procainamide into anionic

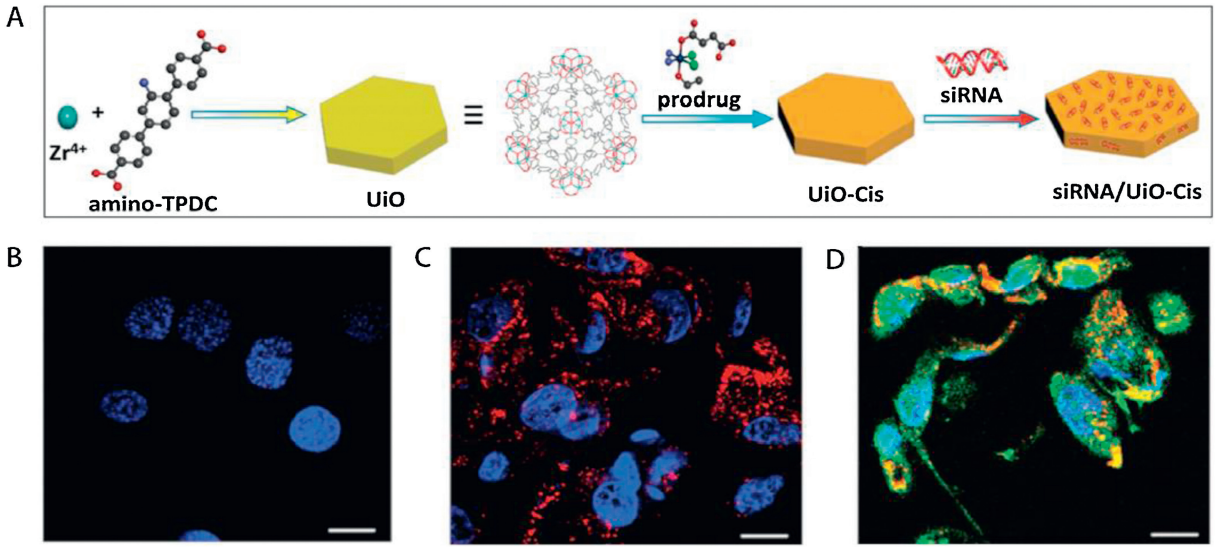

Fig. 2. Synthesis of siRNA/UiO-Cis and drug delivery. (A) Schematic presentation of siRNA/UiO-cis synthesis and drug-loading. (B) CLSM images showing cell apoptosis and siRNA (TAMRA-labeled, red) internalization in SKOV-3 cells after incubation with UiO-Cis. (C) CLSM images showing cell apoptosis and siRNA (TAMRA-labeled, red) internalization in SKOV-3 cells after incubation with siRNA/UiO. (D) CLSM images showing cell apoptosis and siRNA (TAMRA-labeled, red) internalization in SKOV-3 cells after incubation with siRNA/UiO-cis. Scale bar represents 10 nm. Reproduced with permission [63]. Copyright 2014, American Chemical Society.

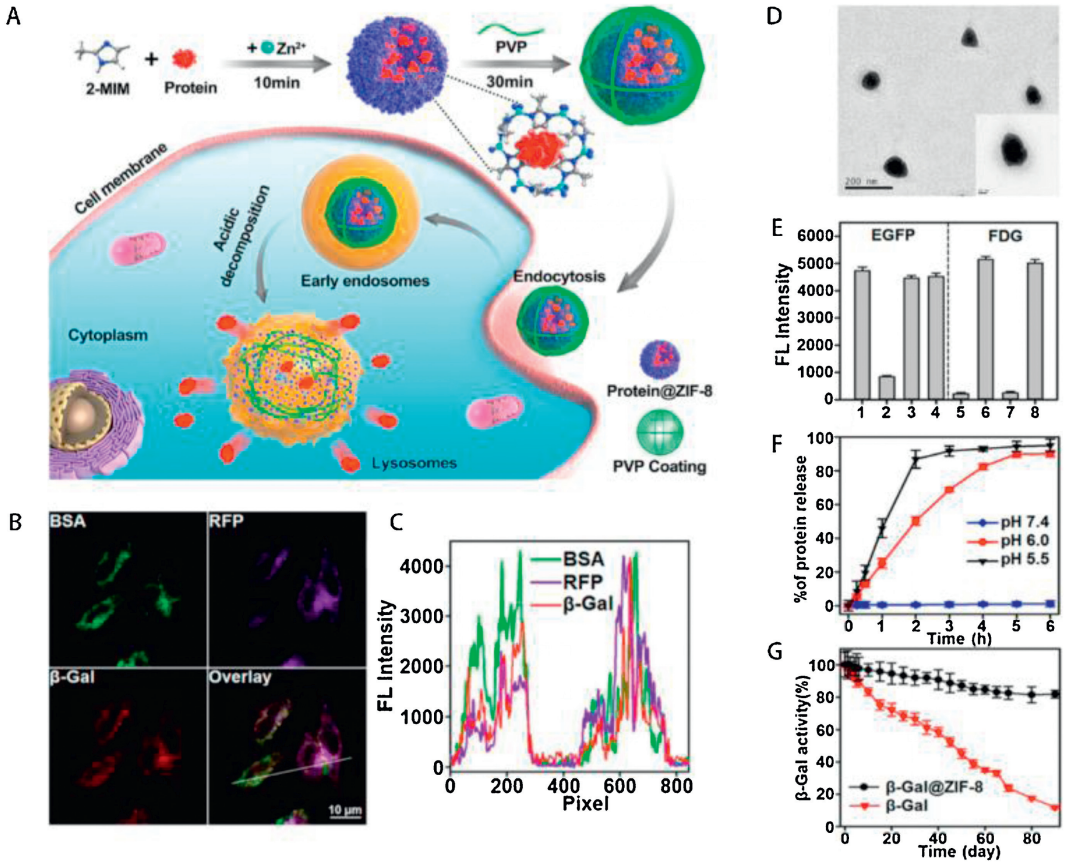

Fig. 3. BSA@ZIF-8 NPs for protein co-delivery in living cells. (A) Illustration of BSA@ZIF-8 NPs for protein delivery in living cells. (B) Fluorescent images of HeLa cells incubated with ZIF-8 NPs encapsulating fluorescein (FITC)-labeled BSA, red fluorescence protein (RFP), and NIR-641-labeled β-Gal. Scale bar: 10 μm. (C) Fluorescence intensity profile of regions of interest (white line). (D) TEM image of PVP-coated BSA@ZIF-8. Scale bar: 200 nm. (E) Protection of ZIF-8-encapsulated proteins. EGFP (1), EGFP + proteases (2), EGFP@ZIF-8+proteases (3), EGFP released from EGFP@ZIF-8 (4), FDG (5), FDG+β-Gal (6), FDG+β-Gal treated by proteases (7), FDG+β-Gal released from β-Gal@ZIF-8 treated by proteases (8). (F) EGFP release from PVP-coated EGFP@ZIF-8. (G) Longterm activity of β-Gal and β-Gal in β-Gal@ZIF-8. Reproduced with permission [101]. Copyright 2018, American Chemical Society.

bio-MOF-1 successfully [96]. The loading of procainamide was 18 wt% and only 20% of the loaded drug was released from bio-MOF-1 after 3 days in neutral PBS. In the subsequent study, An *et al.* investigated the drug loading and releasing property of four bio-MOFs (bio-MOF-1, bio-MOF-4, bio-MOF-100, and bio-MOF-102) [105]. The results showed an initial burst release in all the bio-MOF groups, followed by progressive release for a long period ranging from 49 to 80 days. In addition, numbers of researchers have studied bio-MOFs to explore their potential in drug delivery [106–111]. Sun *et al.* reported the incorporation of the antineoplastic drug dinuclear gold(I) pyrrolidinedithiocarbamato into bio-MOF ZnBTCA [106]. Because of the biodegradability of bio-MOFs, the loaded drug exhibited a sustained releasing mode. The *in vitro* anticancer activities showed that the formed complex had potent anticancer effect, but still cytotoxic to the normal MDCK cells at relatively high concentrations. Recently, Abazari *et al.* synthesized a pH-responsive and tumor-selective system for delivering the DOX through a bio-MOF with a chitosan coating [109]. However, few literatures have been reported on the toxicity, pharmacokinetics and biodistribution of bio-MOFs *in vivo*, further efforts are required in the future research for evaluating and understanding the bio-safety of these emerging materials.

3.2. Biological imaging

The biomedical imaging technologies have been developed rapidly, which facilitated the earlier diseases diagnosis and enabled noninvasive monitoring of the therapeutic processes. In recent years, nMOFs are proved to be emerging imaging agents for producing signals or enhancing signal contrast at targeted sites due to their diverse structures, sizes and metal connecting nodes. These nanoparticles preferred to accumulate in tumor sites because of the EPR effect or tumor-targeting molecules combined to the particles. As a result, nMOFs can be used to diagnose diseases such as various cancers through optical imaging (OI), X-ray computed tomography (CT), magnetic resonance imaging (MRI), and positron emission tomography (PET). The nMOFs can also incorporate different fluorophores to perform intracellular imaging.

3.2.1. Optical imaging

Optical imaging (OI), an imaging modality that uses light illumination to obtain real-time visualization noninvasively, has become a common means to improve surgical outcomes and perform minimally invasive operations. Despite the benefits of OI for the patients, limitations are still obvious such as the shallow penetration of light. Therefore, many fluorescent materials were employed to modify the agents for deep tissues imaging and intracellular imaging [112–116]. For example, Li *et al.* established a new luminescent/magnetic dual-mode imaging method *via* core-shell nanocomposites [114]. The prepared nanomaterials can be selectively uptake by the KB cell lines *in vitro* and the *in vivo* optical imaging and MRI studies exhibited an obvious contrast in KB tumor at 24 h post-injection. In another research, Cai *et al.* incorporated indocyanine green (ICG), a near-infrared (NIR) dye, into MIL-100(Fe) nMOFs with a high loading capacity of 40 wt% and

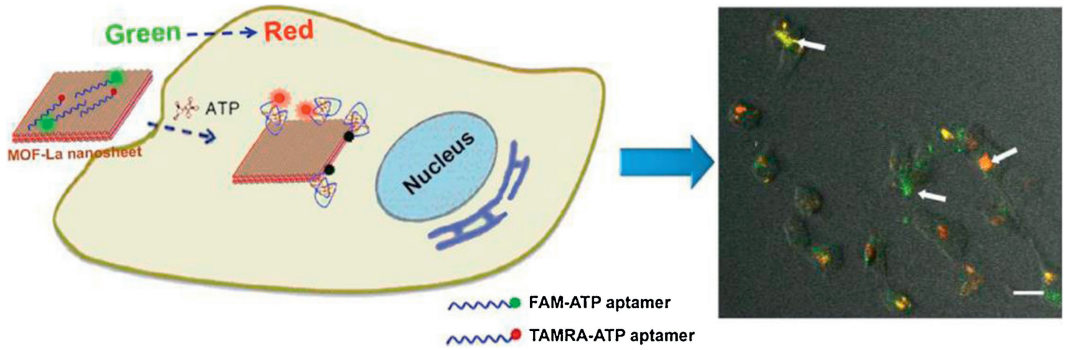

Fig. 4. Intracellular fluorescent imaging of adenosines based on MOF-La nanosheet. Reproduced with permission [117]. Copyright 2017, Nature Publishing Group.

a layer of hyaluronic acid (HA) was coated for tumor-targeting [115]. The prepared particles exhibited a strong NIR absorbance, photostability and high cellular uptake in CD44+ MCF-7 cells both *in vitro* and *in vivo* [114–116].

Recently, several nMOFs have been reported as intracellular bioimaging platforms *via* fluorescent dye-labeled oligonucleotides. For instance, Xia and co-workers formed an ultrathin La-MOF nanosheet for DNA sensing and imaging, and in the subsequent studies, they synthesized a Dye-P2 + MOF-La complex to monitor adenosine in single cells [117]. Fig. 4 showed that the different cells exhibited various fluorescence colors changing from green to red, so that the ATP activity can be observed clearly in different cells. On the other hand, some nMOFs were used for intracellular pH imaging [118–123]. Lin *et al.* synthesized a UiO nMOF through hydrothermal method, and then the pH-dependent ratiometric sensor, fluorescein isothiocyanate (FITC), was conjugated to the formed nMOFs covalently [123]. *In vitro* tests suggested that the F-UiO nMOFs showed an efficient, rapid endocytosis and distributed in the endosomes with integrated structure. As shown in Fig. 5, the fluorescence colors were changed under different pH levels.

3.2.2. X-ray computed tomography

CT is a noninvasive imaging technique for 3D visualization of internal structures based on the attenuation of X-rays and a series of tomographic images are obtained at different orientations. For clinical applications, traditional small molecular contrast agents may cause adverse effects in some patients due to the high doses. Therefore, several functional nMOFs with specific distribution and relatively slow clearance rate have become the potential CT contrast agents [36,124–126]. For example, Zhang *et al.* developed photoactive iodine-boron-dipyrromethene-MOF nanocrystals (UiO-PDT) and demonstrated the potential of these materials to be CT contrast agents [125]. *In vitro* tests suggested the nanocrystals have excellent cytocompatibility and *in vivo* toxicity assessment showed negligible toxicity even at a high dose of 100 mg/kg. At 24 h post-injection, the materials mainly accumulated in tumor sites and the shape of the tumor was clearly distinguished from adjacent tissues. Recently, Han and coworkers explored novel lactobionic acid (LA) modified-MOF Janus nanoparticles (LA-AuNR/ZIF-8 JNP) with DOX loaded for CT image-guided liver cancer therapy [36]. The formed nanocompounds

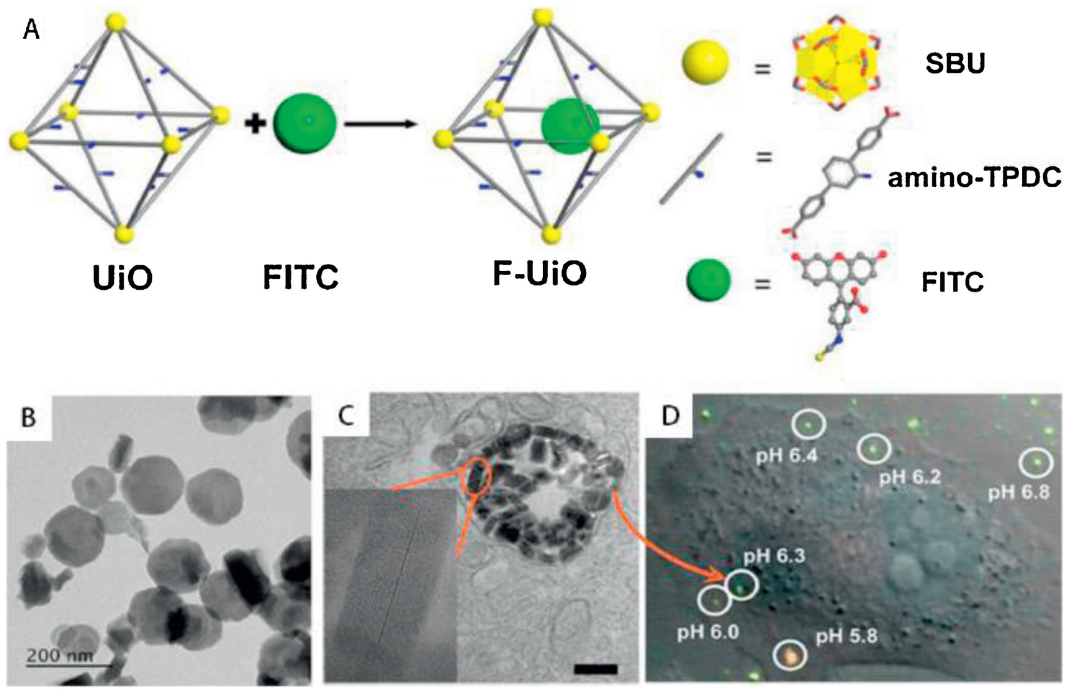

Fig. 5. F-UiO NMOFs for real-time intracellular pH sensing. (A) Schematic presentation of F-UiO synthesis; (B) TEM image of the morphology of F-UiO. (C) Cellular uptake and intracellular distribution of F-UiO in H460 cells. (D) The pH imaging in living cells. Reproduced with permission [123]. Copyright 2014, American Chemical Society.

could be used as CT imaging contrast agents due to the strong X-ray attenuation of AuNRs. *In vitro* and *in vivo* studies showed that the LA-AuNR/ZIF-8 JNPs possessed the tumor-targeting property as well as the anti-cancer effect with fewer side effects.

3.2.3. Magnetic resonance imaging

Magnetic resonance imaging (MRI), a promising non-invasive diagnostic technique based on nuclear magnetic resonance of atoms in the body and the absorption and transmission of high-frequency radio waves are analyzed to produce computerized images. MRI provides a powerful method to diagnose various diseases such as cancer *via* reducing longitudinal (T_1) and transverse (T_2) relaxation time of water protons in the target soft tissue. The ideal contrast agents are preferred to be chemically stable, release almost none of the metal ion in the body and easy to be modified with super-paramagnetic nanoparticles and targeting molecules. Therefore, Mn-based MOFs, Fe-based MOFs and Gd-based MOFs are able to provide potential candidates for MRI applications [127–135]. For example, Lin *et al.* first reported Gd^{3+}-containing nMOFs as T_1-weighted contrast agents with an r_1 relaxivity of 35.8 L $mmol^{-1}$ s^{-1} per Gd^{3+} and $\sim 1.6 \times 10^7$ L $mmol^{-1}$ s^{-1} on a per nMOF basis [135]. Recently, some studies focused on the syntheses of nanoparticles for dual-modality imaging. Kundu *et al.* designed two Gd^{3+}-based fluorescent porous MOFs for fluorescence imaging and MRI without the incorporation of fluorescent linker molecules [132]. The two formed MOFs were both proved to be potential T_1-weighted MRI contrast agents with good longitudinal relaxivity.

Taking account of the toxicity of Gd^{3+}, the Mn-based MOFs and Fe-based MOFs are considered to be better contrast agents for MRI because of their lower toxicity and the efficient T_1-weighted contrast enhancement when binding to intracellular proteins. For instance, Yang *et al.* developed Mn^{2+}-based nMOFs with IR825, a NIR dye, to obtain the photothermal therapeutic effect [136]. *In vitro* and *in vivo* tests showed that the IR825@Mn^{2+}-based nMOFs possessed MRI ability as well as effective photothermal ablation of tumor.

In addition, the nMOFs-based MRI contrast agents can incorporate variety drugs for therapeutics, which is superior to the conventional agents. Fu *et al.* synthesized a novel Fe_3O_4@UiO-66 core-shell composite with high drug loading capacity (63 wt%) and high transverse relaxivity (255.87 L $mmol^{-1}$ s^{-1}) for cancer diagnosis and therapy [129]. *In vivo* biodistribution study showed that the major accumulation was in the spleen and liver, which was in accord with the T_2-weighted MR images. And a long-term toxicity assessment indicated that no obvious disorder was observed in major organs after injection for 30 days. These results suggested that the nMOFs are promising candidates for the future MRI application and clinical translation.

3.2.4. Positron emission tomography

Positron emission tomography (PET) is an imaging technique in nuclear medicine that provides high-resolution 3D images of metabolic processes in the body *via* recording the emission of positrons from radioactive substances accumulating at the target organs or tissues. In comparison to other bioimaging techniques, PET possesses deeper signal penetration, higher detection sensitivity and superior quantitation ability. As shown in Fig. 6, Hong *et al.* designed an ^{89}Zr-containing nMOF for PET imaging [65]. *In vitro* tests suggested that the prepared nanomaterials have good radiochemical stability and material integrity. The distribution of UiO-66/Py-PGA-PEG-F3 was traced through PET scans and an obvious signal was captured in tumor site at 2 h after injection. The nanoparticles also accumulated in the liver and spleen, but no obvious uptake was noticed in the kidney or bone. The toxicity evaluation of ^{89}Zr-UiO-66 conjugates *in vivo* showed that no significant toxicity was caused in the experimental groups even at a high dose of 50 mg/kg for 30 days. These results indicated that the ^{89}Zr-based nMOFs are potential materials for long-term PET imaging and combinational radiation/chemotherapy.

3.3. Biosensing

Another up-to-date application of nMOFs is to probe physiological processes as biosensors because of their wide applicability in different biological systems. The types and concentrations of metabolites in cells are changing with the physiological environments, thus the sensitive biosensors are helpful for diseases

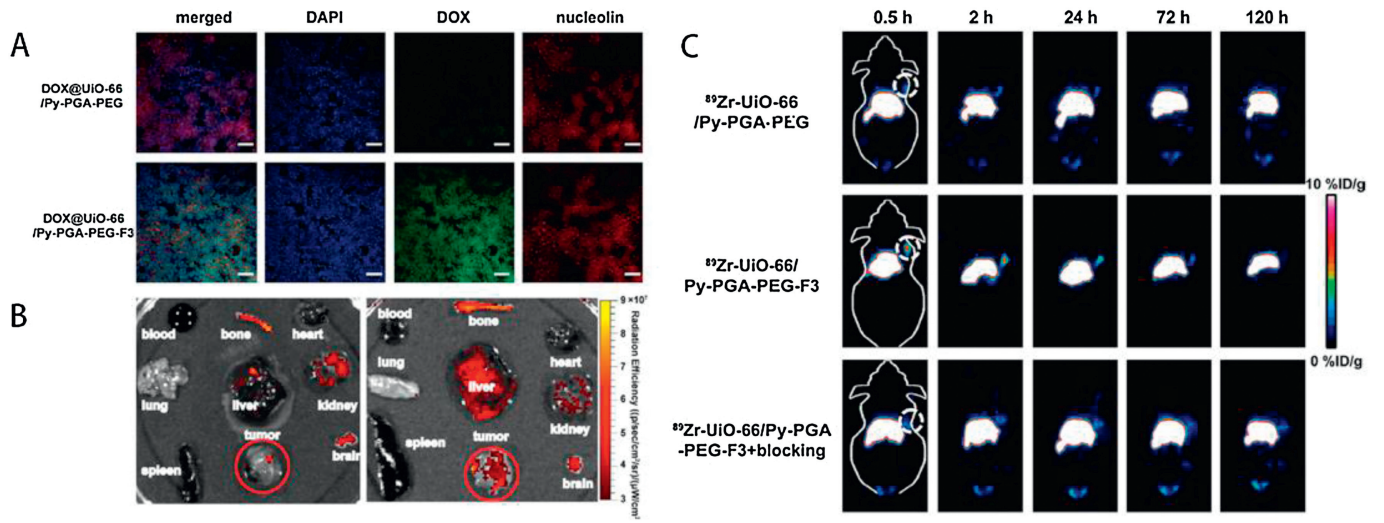

Fig. 6. Drug delivery and PET images of ^{89}Zr-UiO-66 nMOFs *in vitro* and *in vivo*. (A) Immunohistological staining of MDA-MB-231 tumors from mice injected with DOX@UiO-66/Py−PGA-PEG-F3 and DOX@UiO-66/Py−PGA-PEG. Nucleolin (red) expression profile was compared with DOX (green) distribution pattern from both of the UiO-66 conjugates. Scale bar: 100 μm. (B) *Ex vivo* fluorescence images of DOX in the major organs/tissues at 2 h after intravenous injection of DOX@UiO-66/Py-PGA-PEG-F3 and DOX@UiO-66/Py-PGA-PEG. (C) Representative coronal PET images of MDA-MB-231 tumor bearing mice at different time point's post-injection of ^{89}Zr-UiO-66/Py-PGA-PEG-F3, ^{89}Zr-UiO-66/Py-PGA-PEG, and ^{89}Zr-UiO-66/Py-PGA-PEG-F3 with excessive amount of F3 peptide blocking. The location of tumors was identified by dashed circles. Reproduced with permission [64]. Copyright 2017, American Chemical Society.

diagnosis. Compared to conventional small molecular biosensors, nMOF-based biosensors overcome many disadvantages, such as the leaching and self-quenching, to obtain high resolution, high sensitivity and high accuracy properties for subcellular sensing. Some current studies have reported the cellular and subcellular sensing of several nMOF-based biosensors, including DNA and RNA sensing, intracellular molecules sensing, intracellular pH sensing and intracellular temperature sensing.

3.3.1. Nucleic acid sensing

DNAs and RNAs play an important role in physiological regulation, so the levels of nucleic acid can help diagnose diseases and monitor biological processes. Chen and co-workers first reported the incorporation of triplex-forming oligonucleotide with H_2dtoaCu nMOFs for the detection of HIV DNA sequences [74]. In the following studies, they designed various nMOFs to sense virus DNA or RNA [84,137–142]. For instance, they modified carboxy-fluorescein (FAM)-labeled probe ss-DNA on the nMOFs to detect HIV ds-DNA and SUDV RNA. The fluorescence of FAM can be recovered when the formed biosensor reacted with the target DNA or RNA, thus it can be served as an effective, fluorescent-sensing platform. Besides, Huskens *et al.* prepared a peptide nucleic acid (PNA)-functionalized MIL-88A nMOFs through covalent and non-covalent method for distinguishing single-base mismatched or random sequences from the complementary DNA *via* flow cytometry using immunofluorescence technique [143]. The formed biosensing system was proved to bind with DNA selectively and the DNA-PNA duplex could enhance the difference between the targeted DNA.

3.3.2. Intracellular molecules sensing

Small-biomolecules such as gas molecules, glucose and metal ions in the tissue can reflect many diseases due to their indispensable role in physiological activities. Lin *et al.* first reported the R-UiO based bio-MOF as a phosphorescence/fluorescence dual-emissive platform to quantify the intracellular oxygen ratio [144]. The Pt(II)-porphyrin ligand (Pt-5,15-di(*p*-benzoato)porphyrin (DBP-Pt)) was served as an oxygen-responsive probe, and the rhodamine B isothiocyanate ligand was taken as an oxygen-independent reference probe. *In vitro* tests suggested that the R-UiO based bio-MOFs can be used as oxygen biosensors in live-cells.

Wei *et al.* synthesized a nanocomposite *via* conjugating gold nanoparticles (GNPs) and glucose oxidase (GOx) with MIL-101 nMOFs to measure glucose and lactate in living-tissues [145]. The glucose and lactate can be quantified *via* surface enhanced Raman scattering and this study showed that the formed nanomaterial can be used as a novel diagnostic platform for ischemic stroke (Fig. 7).

In addition, several investigations related to metal ions detection have been reported [146–149]. Lu *et al.* designed three different nMOF-253s for Fe^{2+} sensing due to their excellent

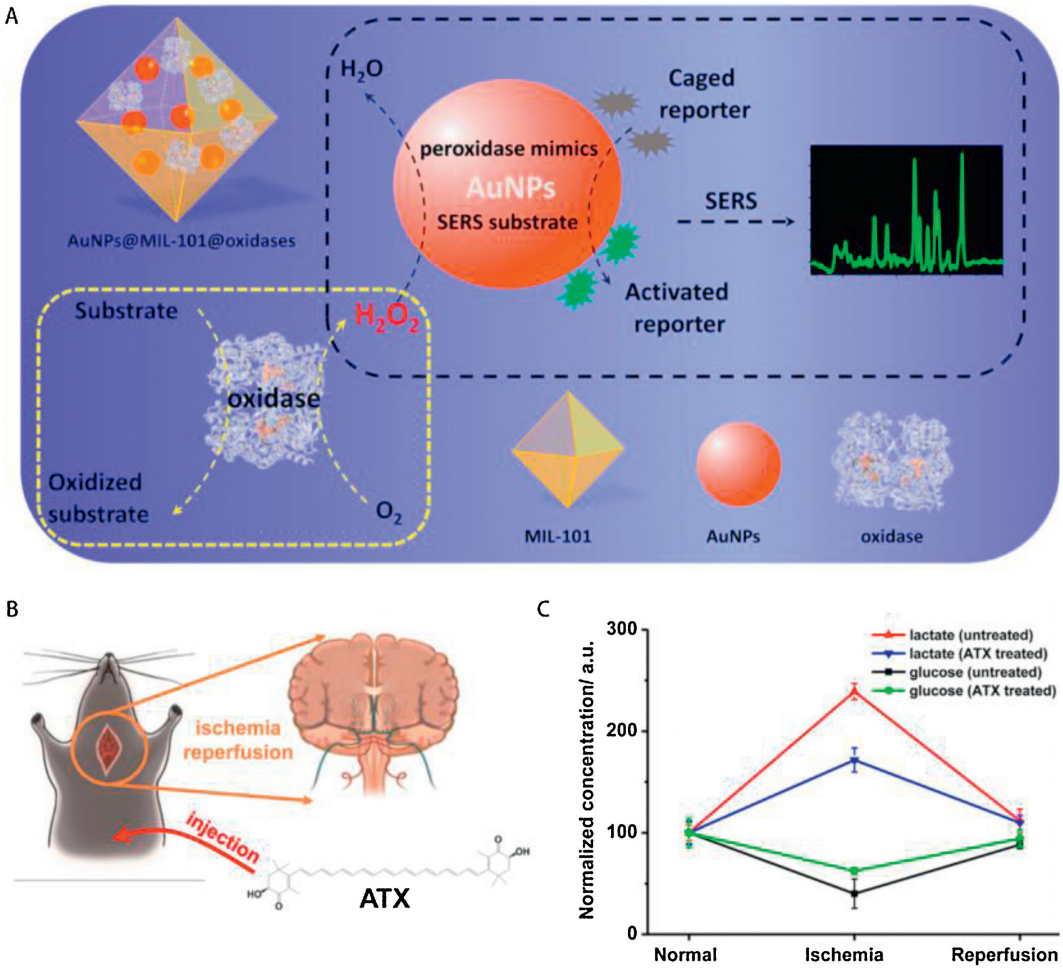

Fig. 7. Monitoring glucose and lactate in living brains and evaluating the therapeutic efficacy of ATX. (A) Schematic illustration of AuNPs@MIL-101@oxidases for efficient enzymatic cascade reactions. (B) Schematic illustration of global cerebral ischemia/reperfusion and the treatment with ATX. (C) Dynamic changes of glucose and lactate following ischemia and reperfusion with and without ATX pretreatment. The glucose and lactate levels before ischemia were normalized as 100. Reproduced with permission [145]. Copyright 2017, American Chemical Society.

fluorescent quenching specificity for ferric ion [146]. Among the three nMOF-253s, nMOF-253(γ) are able to be transferred into HeLa cells so that it can be a potential biosensor for intracellular Fe^{2+} detection.

3.3.3. Intracellular pH sensing

Intracellular pH can reflect the changes of physiological environments and the anomalous changes of intracellular pH are generally concerned in drug-resistance or tumorigenesis. Lin *et al.* first developed F-UiO nMOFs for real-time intracellular pH sensing by conjugating fluorescein isothiocyanate with the Zr-based nMOFs [124]. The formed nanoparticles exhibited well fluorescence and pH-sensing property. After uptake by the live cells, the nanoparticles remained structural integrity in the endosomes and the acidification of endosomes was reflected *via* confocal microscopy imaging. This study provided a new nanosensor for intracellular pH sensing and offered new insights into the nMOF-cell interactions.

3.3.4. Intracellular temperature sensing

Interestingly, Zhao and coworkers reported a new thermosensitive near-infrared LnMOF in 2016 [150]. The formed LnMOFs showed outstanding temperature dependence photoluminescence properties within the physiological range of 303 – 333 K and the temperature resolution is 0.0096 K, which enable the detection of temperature difference between normal cells and major pathological cells.

3.4. Biocatalysis

Another notable application of nMOFs is biomimetic catalysis. Because of their nanoscale structure, some specific nMOFs possess both highly efficient catalysis and relatively low toxicity properties. In comparison to the natural enzymes, these enzymatic mimic nMOFs are easier and cheaper to synthesize and have better chemical stability. Therefore, these nMOFs can be served as potential candidates for medical diagnose and immunoassay [151–155]. For example, Zhang *et al.* reported a nanometric MIL-100, which performed the intrinsic peroxidase-like catalytic activity, for ascorbic acid colorimetric sensing [151]. The prepared nMOFs catalyzed the oxidation of different peroxidase substrates by H_2O_2 and caused the obvious color change of the solution. The catalysis of this nMOFs strongly depended on H_2O_2 concentration, temperature and pH level. Recently, Wu and coworkers synthesized a metalloporphyrin-bioMOF as tri-component biomimetic catalyst platform consisting of sandwich-type polyoxometallate and *N*-hydroxyphthalimide [152–154]. The studies on aerobic oxidation of ethylbenzene showed that the formed nanoparticles could immensely enhance the oxidation reaction under mild conditions and had sustainability and notable selectivity for the efficient biomimetic activation.

The MOFs can be utilized to immobilize enzymes and perform biocatalytic functions. Ma *et al.* first reported the successful immobilization of microperoxidase-11 (MP-11) into the mesoporous MOFs and the MP-11@Tb-mesoMOFs showed a better catalytic capacity compared with the previous MP-11 [156]. In the following studies, they encapsulated the heme protein Cyt c into the channels of Tb-TATB MOFs despite the relatively bulky volume of Cyt c molecules [157]. Wu and coworkers synthesized a catalytic ZIF-8 with two enzymes immobilized, including FITC-labelled glucose oxidase (GOx) and horseradish peroxidase (HRP), for detecting glucose in cells [158]. The GOx&HRP/ZIF-8 nanocomposite displayed high catalytic efficiency, excellent selectivity and thermal stability.

Besides the above-mentioned bio-applications of nMOFs, some novel researches are also been reported recently. For example, some researchers have studied the osteogenesis promotion ability of several nMOFs [109,159,160]. Pei *et al.* successfully fabricated a ZIF-8 coating on the surface of heat-treated titanium (AHT) implants [159]. The results of *in vitro* tests showed that the ZIF-8@AHTs not only improved extracellular matrix mineralization and collagen secretion, but up-regulated the expression of osteogenic genes as well. Meanwhile, the ZIF-8@AHTs implants showed a better osseointegration than the Ti and AHT implants *in vivo*. Moreover, Abazari and co-workers synthesized a magnetic bio-metal-organic framework and studied its anti-leishmanial effect *in vitro* and *in vivo* [161]. They straightforwardly synthesized magnetic Fe_3O_4@bio-MOFs using adenine as organic linkers and zinc as metal ion and the results of various experiments *in vitro* and *in vivo* showed that their anti-leishmanial behavior are positively related to the exposure time and dose concentration.

4. Conclusions and prospects

Significant progress has been made for nMOFs in many fields in the past decades, and various functionalization methods were performed to enhance the applicability and multiply the functionality of nMOFs. Because of their high porosity, wide range of pore shapes, large surface area, nanoscale size and tunable structures, the nMOFs have become potential materials for numerous biological applications such as drug delivery, bioimaging, biosensing and biocatalysis. In this review, we summarized the up-to-date progresses of nMOFs, including the common surface modification methods and the developments in bioapplication fields.

As described here, plenty of notable nMOF-based platforms have been designed ranging from individual nanoparticles to functional composite systems. However, much more efforts should be made in the future research related to the stimuli-responsive release mechanisms, imaging/sensing/catalytic efficacy, pharmacokinetics and biodistribution, biocompatibility and toxicology of nMOFs. Firstly, as for the synthesis of nMOFs, much more attention should be paid to the nontoxic or low-toxicity raw materials and mild reaction conditions. Bioactive substance as the ingredients and modifications are considered to be essential to achieve these requirements. For example, constitutive part of body components and endogenous building blocks can be served as organic linkers due to their lower toxicity compared to the traditional chemical materials, and probably reduce the side effects of nMOFs. Introducing biological molecules into the frameworks and surface of nMOFs are potential methods to facilitate the clinical application of these materials. Secondly, further studies on the biological applications are needed. Stability, degradability, blood circulation half-life and selectivity are essential intrinsic properties of the nMOFs to function in the body and the final controlled-releasing/imaging/sensing/catalytic efficacy varies with these different properties. So far, no systematic comparison has been reported on the efficiency of these functional nMOFs, which limits the comprehensive understanding of their properties for biological applications. Thirdly, much effort should be devoted to the biocompatibility and toxicology of nMOFs. Studies on the *in vivo* toxicity, pharmacokinetics and biodistribution of many new nMOFs are currently inadequate, which are basics of preclinical biocompatible assessments of these emerging materials. In addition, the administration routes (oral administration, intravenous administration or intraabdominal administration), the age of experimental animals (embryos, neonatal animals or adult animals) and the physiological status of experimental animals (pregnant or not) are also need to be investigated in the future. Finally, a comprehensive understanding of the reaction and metabolism mechanism is required to improve the performance of nMOFs before clinical application. The nanoscale MOFs will certainly become one of the most promising materials in the

biomedical field in the next decade, and we hope this review can provide new approach to move this field forward.

Declaration of competing interest

The authors declare no conflict of interest.

Acknowledgments

This research was supported by the National Natural Science Foundation of China (Nos. 81970985, 81771122, 81601613, 21501123), Science & Technology Support Program of Sichuan Province (Nos. 2018SZ0037, 19YYJC2625), the Graduate Student's Research and Innovation Fund of Sichuan University (No. 2018YJSY108), the China Postdoctoral Science Foundation Funded Project (No. 2018M640931), and the Science & Technology Key Research and Development Program of Sichuan Province (No. 2019YFS0142).

References

[1] B.F. Hoskins, R. Robson, J. Am. Chem. Soc. 111 (1989) 5962–5964.
[2] H. Furukawa, K.E. Cordova, M. O'Keeffe, et al., Science 341 (2013) 1230444.
[3] M. Eddaoudi, J. Kim, N. Rosi, et al., Science 295 (2002) 469–472.
[4] M.P. Suh, H.J. Park, T.K. Prasad, et al., Chem. Rev. 112 (2012) 782–835.
[5] K. Sumida, D.L. Rogow, J.A. Mason, et al., Chem. Rev. 112 (2012) 724–781.
[6] J.R. Li, J. Sculley, H.C. Zhou, Chem. Rev. 112 (2012) 869–932.
[7] Y. He, W. Zhou, G. Qian, B. Chen, Chem. Soc. Rev. 43 (2014) 5657–5678.
[8] J.R. Li, J. Yu, W. Lu, et al., Nat. Commun. 4 (2013) 1538.
[9] X. Guan, Y. Wang, W.F. Cai, Chin. Chem. Lett. 30 (2019) 1310–1314.
[10] S. Wang, Z.W. Ma, X.Y. Du, et al., Mater. Express 8 (2018) 381–387.
[11] Y. Wang, L.J. Li, L.T. Yan, et al., Chin. Chem. Lett. 29 (2018) 849–853.
[12] J. Liu, L. Chen, H. Cui, et al., Chem. Soc. Rev. 43 (2014) 6011–6061.
[13] J.S. Seo, D. Whang, H. Lee, et al., Nature 404 (2000) 982–986.
[14] J. Lee, O.K. Farha, J. Roberts, et al., Chem. Soc. Rev. 38 (2009) 1450–1459.
[15] L. Ma, J.M. Falkowski, C. Abney, W. Lin, Nat. Chem. 2 (2010) 838–846.
[16] M. Zhao, S. Ou, C.D. Wu, Acc. Chem. Res. 47 (2014) 1199–1207.
[17] A. Corma, H. García, F.X. Llabrés i Xamena, Chem. Rev. 110 (2010) 4606–4655.
[18] X.L. Lv, K. Wang, B. Wang, et al., J. Am. Chem. Soc. 139 (2017) 211–217.
[19] R.J. Wu, M. Liu, Y.W. Peng, et al., Chin. Chem. Lett. 30 (2019) 989–994.
[20] K. Li, K.H. He, Q.W. Li, et al., Chin. Chem. Lett. 30 (2019) 499–501.
[21] X.Y. Ren, L.H. Lu, Chin. Chem. Lett. 26 (2015) 1439–1445.
[22] M. Kurmoo, Chem. Soc. Rev. 38 (2009) 1353–1379.
[23] T. Zhang, W. Lin, Chem. Soc. Rev. 43 (2014) 5982–5993.
[24] C.A. Kent, B.P. Mehl, L. Ma, et al., J. Am. Chem. Soc. 132 (2010) 12767–12769.
[25] J.L. Wang, C. Wang, W. Lin, ACS Catal. 2 (2012) 2630–2640.
[26] P. Ling, J. Lei, L. Zhang, H. Ju, Anal. Chem. 87 (2015) 3957–3963.
[27] P. Ling, J. Lei, H. Ju, Biosens. Bioelectron. 71 (2015) 373–379.
[28] A. Samui, K. Pal, P. Karmakar, S.K. Sahu, Mater. Sci. Eng. C-Mater. Biol. Appl. 98 (2019) 772–781.
[29] K.M. Taylor-Pashow, J. Della Rocca, Z. Xie, et al., J. Am. Chem. Soc. 131 (2009) 14261–14263.
[30] P. Horcajada, T. Chalati, C. Serre, et al., Nat. Mater. 9 (2010) 172–178.
[31] X. Zhang, L. Fang, K. Jiang, et al., Biosens. Bioelectron. 130 (2019) 65–72.
[32] P. Horcajada, C. Serre, G. Maurin, et al., J. Am. Chem. Soc. 130 (2008) 6774–6780.
[33] P. Jiang, Y. Hu, G. Li, Talanta 200 (2019) 212–217.
[34] X.Y. Lai, H. Liu, Y.T. Zheng, et al., J. Biomed. Nanotechnol. 15 (2019) 1754–1763.
[35] B. Yang, M. Shen, J. Liu, F. Ren, Pharm. Res. 34 (2017) 2440–2450.
[36] H. Zhang, Q. Zhang, C. Liu, B. Han, Biomater. Sci. 7 (2019) 1696–1704.
[37] M.X. Wu, Y.W. Yang, Adv. Mater. 29 (2017) 1606134.
[38] P. Horcajada, C. Serre, M. Vallet-Regi, et al., Angew. Chem. Int. Ed. 45 (2006) 5974–5978.
[39] K. Deng, Z. Hou, X. Li, et al., Sci. Rep. 5 (2015) 7851.
[40] R. Ricco, W. Liang, S. Li, et al., ACS Nano 12 (2018) 13–23.
[41] M. Gimenez-Marques, M.L. Garcia-Sanz de Larrea, E. Coronado, J. Mater. Chem. C-Mater. 3 (2015) 7946–7953.
[42] C. Doonan, R. Ricco, K. Liang, et al., Acc. Chem. Res. 50 (2017) 1423–1432.
[43] M. Lismont, L. Dreesen, S. Wuttke, Adv. Funct. Mater. 27 (2017) 1606314.
[44] G. Lan, K. Ni, W. Lin, Coord. Chem. Rev. 379 (2019) 65–81.
[45] B. Pelaz, C. Alexiou, R.A. Alvarez-Puebla, et al., ACS Nano 11 (2017) 2313–2381.
[46] C.E. O'Hanlon, K.G. Amede, M.R. O'Hear, J.M. Janjic, J. Fluor. Chem. 137 (2012) 27–33.
[47] M. Liong, J. Lu, M. Kovochich, et al., ACS Nano 2 (2008) 889–896.
[48] K.C. Leung, C.H. Wong, X.M. Zhu, et al., Quant. Imag. Med. Surg. 3 (2013) 302–307.
[49] X.M. Zhu, J. Yuan, K.C. Leung, et al., Nanoscale 4 (2012) 5744–5754.
[50] M.T. Simon-Yarza, T. Baati, A. Paci, et al., J. Mater. Chem. B 4 (2016) 585–588.
[51] Y.H. Kiang, G.B. Gardner, S. Lee, et al., J. Am. Chem. Soc. 121 (1999) 8204–8215.
[52] J. Canivet, S. Aguado, G. Bergeret, D. Farrusseng, Chem. Commun. 47 (2011) 11650–11652.
[53] W. Morris, W.E. Briley, E. Auyeung, et al., J. Am. Chem. Soc. 136 (2014) 7261–7264.
[54] J.S. Kahn, L. Freage, N. Enkin, M.A. Garcia, I. Willner, Adv. Mater. 29 (2017) 1602782.
[55] Y.H. Shih, S.H. Lo, N.S. Yang, et al., ChemPlusChem 77 (2012) 982–986.
[56] S. Jung, Y. Kim, S.J. Kim, et al., Chem. Commun. 47 (2011) 2904–2906.
[57] A. Lazaro, S. Haddad, J.M. Rodrigo-Munoz, et al., ACS Appl. Mater. Interfaces 10 (2018) 5255–5268.
[58] L. Kan, Y. Jiang, A.Q. Xue, et al., Inorg. Chem. 57 (2018) 5420–5428.
[59] X.Y. Zhu, J.L. Gu, Y. Wang, et al., Chem. Commun. 50 (2014) 8779–8782.
[60] J. Park, Q. Jiang, D.W. Feng, et al., J. Am. Chem. Soc. 138 (2016) 3518–3525.
[61] R. Roder, T. Preiss, P. Hirschle, et al., J. Am. Chem. Soc. 139 (2017) 2359–2368.
[62] W.Q. Wang, L. Wang, Z.S. Li, Z.G. Xie, Chem. Commun. 52 (2016) 5402–5405.
[63] C.B. He, K.D. Lu, D.M. Liu, W.B. Lin, J. Am. Chem. Soc. 136 (2014) 5181–5184.
[64] D.Q. Chen, D.Z. Yang, C.A. Dougherty, et al., ACS Nano 11 (2017) 4315–4327.
[65] W.J. Ma, Q. Jiang, P. Yu, et al., Anal. Chem. 85 (2013) 7550–7557.
[66] H. Yang, C.Y. Qin, C. Yu, et al., Adv. Funct. Mater. 24 (2014) 1738–1747.
[67] L. Zhang, J.P. Lei, F.J. Ma, et al., Chem. Commun. 51 (2015) 10831–10834.
[68] P.F. Gao, L.L. Zheng, L.J. Liang, et al., J. Mater. Chem. B 1 (2013) 3202–3208.
[69] M. Ferrari, Nat. Rev. Cancer 5 (2005) 161–171.
[70] S. Mitragotri, P.A. Burke, R. Langer, Nat. Rev. Drug Discov. 13 (2014) 655–672.
[71] V. Weissig, T.K. Pettinger, N. Murdock, Int. J. Nanomed. 9 (2014) 4357–4373.
[72] E. Fattal, N. Grabowski, S. Mura, et al., J. Biomed. Nanotechnol. 10 (2014) 2852–2864.
[73] J.R. Long, O.M. Yaghi, Chem. Soc. Rev. 38 (2009) 1213–1214.
[74] R. Millward, O.M. Yaghi, J. Am. Chem. Soc. 127 (2005) 17998–17999.
[75] L. Foo, R. Matsuda, S. Kitagawa, Chem. Mater. 26 (2014) 310–322.
[76] S. Furukawa, J. Reboul, S. Diring, et al., Chem. Soc. Rev. 43 (2014) 5700–5734.
[77] D. Liu, K. Lu, C. Poon, W. Lin, Inorg. Chem. 53 (2014) 1916–1924.
[78] J.L. Vivero-Escoto, R.C. Huxford-Phillips, W. Lin, Chem. Soc. Rev. 41 (2012) 2673–2685.
[79] Y. Ikezoe, J. Fang, T.L. Wasik, et al., Adv. Mater. 27 (2015) 288–291.
[80] Y. Ikezoe, J. Fang, T.L. Wasik, et al., Nano Lett. 15 (2015) 4019–4023.
[81] L. Chen, H. Zheng, X. Zhu, et al., Analyst 138 (2013) 3490–3493.
[82] X.F. Wei, L.Y. Zheng, F. Luo, et al., J. Mater. Chem. B 1 (2013) 1812–1817.
[83] X. Zhu, H.Y. Zheng, X.F. Wei, et al., Chem. Commun. 49 (2013) 1276–1278.
[84] T. Ye, Y.F. Liu, M. Luo, et al., Analyst 139 (2014) 1721–1725.
[85] F.J. Lyu, Y.F. Zhang, R.N. Zare, J. Ge, Z. Liu, Nano Lett. 14 (2014) 5761–5765.
[86] K. Liang, R. Ricco, C.M. Doherty, et al., Nat. Commun. 6 (2015) 7240.
[87] F.K. Shieh, S.C. Wang, C.I. Yen, et al., J. Am. Chem. Soc. 137 (2015) 4276–4279.
[88] H. Cheng, J.Y. Zhu, S.Y. Li, et al., Adv. Funct. Mater. 26 (2016) 7847–7860.
[89] Y.Q. Yin, C.L. Gao, Q. Xiao, et al., ACS Appl. Mater. Interfaces 8 (2016) 29052–29061.
[90] J.D. Cui, Y.X. Feng, T. Lin, et al., ACS Appl. Mater. Interfaces 9 (2017) 10587–10594.
[91] T. Kundu, S. Mitra, P. Patra, et al., Chem. -Eur. J. 20 (2014) 10514–10518.
[92] E. Bellido, T. Hidalgo, M.V. Lozano, et al., Adv. Healthc. Mater. 4 (2015) 1246–1257.
[93] F. Ke, Y.P. Yuan, L.G. Qiu, et al., J. Mater. Chem. 21 (2011) 3843–3848.
[94] M. Nazari, M. Rubio-Martinez, G. Tobias, et al., Adv. Funct. Mater. 26 (2016) 3244–3249.
[95] W.H. Chen, X. Yu, A. Cecconello, et al., Chem. Sci. 8 (2017) 5769–5780.
[96] K.S. Park, Z. Ni, A.P. Cote, et al., Proc. Natl. Acad. Sci. U. S. A. 103 (2006) 10186–10191.
[97] C.Y. Sun, C. Qin, X.L. Wang, et al., Dalton Trans. 41 (2012) 6906–6909.
[98] R.X. Bian, T.T. Wang, L.Y. Zhang, et al., Biomater. Sci.-UK 3 (2015) 1270–1278.
[99] H.J. Zhang, W. Chen, K. Gong, J.H. Chen, ACS Appl. Mater. Inter. 9 (2017) 31519–31525.
[100] X.R. Chen, R.L. Tong, Z.Q. Shi, et al., ACS Appl. Mater. Inter. 10 (2018) 2328–2337.
[101] T.T. Chen, J.T. Yi, Y.Y. Zhao, X. Chu, J. Am. Chem. Soc. 140 (2018) 9912–9920.
[102] X. Zhang, J. Wang, J.X. Wu, et al., J. Biomater. Appl. 34 (2019) 396–407.
[103] J.Y. An, S.J. Geib, N.L. Rosi, J. Am. Chem. Soc. 131 (2009) 8376–8377.
[104] J. An, O.K. Farha, J.T. Hupp, et al., Nat. Commun. 3 (2012) 604.
[105] H. Oh, T. Li, J. An, Chem. -Eur. J. 21 (2015) 17010–17015.
[106] R.W.Y. Sun, M. Zhang, D. Li, et al., Chem. -Eur. J. 21 (2015) 18534–18538.
[107] J. Liu, T.Y. Bao, X.Y. Yang, et al., Chem. Commun. 53 (2017) 7804–7807.
[108] W. Liu, Z.J. Yan, Z.D. Zhang, et al., J. Alloys. Compd. 788 (2019) 705–711.
[109] R. Abazari, A.R. Mahjoub, F. Ataei, et al., Inorg. Chem. 57 (2018) 13364–13379.
[110] V. Nejadshafiee, H. Naeimi, B. Goliaei, et al., Mat. Sci. Eng. C-Mater. 99 (2019) 805–815.
[111] F. Abbasloo, S.A. Khosravani, M. Ghaedi, et al., Ultrason. Sonochem. 42 (2018) 237–243.
[112] M.D. Rowe, D.H. Thamm, S.L. Kraft, S.G. Boyes, Biomacromolecules 10 (2009) 983–993.
[113] R. Nishiyabu, N. Hashimoto, T. Cho, et al., J. Am. Chem. Soc. 131 (2009) 2151–2158.
[114] Y.T. Li, J.L. Tang, L.C. He, et al., Adv. Mater. 27 (2015) 4075–4080.
[115] W. Cai, H.Y. Gao, C.C. Chu, et al., ACS Appl. Mater. Interfaces 9 (2017) 2040–2051.
[116] W. Liu, Y.M. Wang, Y.H. Li, et al., Small 13 (2017) 1603459.
[117] H.S. Wang, J. Li, J.Y. Li, et al., NPG Asia Mater. 9 (2017) e354.
[118] Y.K. Huang, B.X. Liu, Q. Shen, et al., Talanta 164 (2017) 427–431.
[119] Y. Lu, B. Yan, Chem. Commun. 50 (2014) 13323–13326.

[120] Y.S. Yang, K.Z. Wang, D.P. Yan, ACS Appl. Mater. Interfaces 8 (2016) 15489–15496.
[121] M.H. Zeng, Z. Yin, Z.H. Liu, et al., Angew. Chem. Int. Ed. 55 (2016) 11407–11411.
[122] L. He, T.T. Wang, J.P. An, et al., CrystEngComm 16 (2014) 3259–3263.
[123] C.B. He, K.D. Lu, W.B. Lin, J. Am. Chem. Soc. 136 (2014) 12253–12256.
[124] K.E. deKrafft, W.S. Boyle, L.M. Burk, et al., J. Mater. Chem. 22 (2012) 18139–18144.
[125] T. Zhang, L. Wang, C. Ma, et al., J. Mater. Chem. B 5 (2017) 2330–2336.
[126] W.T. Shang, C.T. Zeng, Y. Du, et al., Adv. Mater. 29 (2017) 1604381.
[127] W.J. Rieter, K.M.L. Taylor, H.Y. An, et al., J. Am. Chem. Soc. 128 (2006) 9024–9025.
[128] Z.Y. Shi, C.C. Chu, Y. Zhang, et al., J. Biomed. Nanotechnol. 14 (2018) 1934–1943.
[129] H.X. Zhao, Q. Zou, S.K. Sun, et al., Chem. Sci. 7 (2016) 5294–5301.
[130] D.D. Wang, J.J. Zhou, R.H. Chen, et al., Biomaterials 100 (2016) 27–40.
[131] D.D. Wang, J.J. Zhou, R.H. Chen, et al., Biomaterials 107 (2016) 88–101.
[132] T. Kundu, S. Mitra, D.D. Diaz, R. Banerjee, ChemPlusChem 81 (2016) 728–732.
[133] M.D. Rowe, C.C. Chang, D.H. Thamm, et al., Langmuir 25 (2009) 9487–9499.
[134] K.M.L. Taylor, A. Jin, W.B. Lin, Angew. Chem. Int. Ed. 47 (2008) 7722–7725.
[135] K.M.L. Taylor, W.J. Rieter, W.B. Lin, J. Am. Chem. Soc. 130 (2008) 14358–14359.
[136] Y. Yang, J.J. Liu, C. Liang, et al., ACS Nano 10 (2016) 2774–2781.
[137] S.P. Yang, S.R. Chen, S.W. Liu, et al., Anal. Chem. 87 (2015) 12206–12214.
[138] L. Qin, L.X. Lin, Z.P. Fang, et al., Chem. Commun. 52 (2016) 132–135.
[139] H.Q. Zhao, G.H. Qiu, Z. Liang, et al., Anal. Chim. Acta 922 (2016) 55–63.
[140] H.Q. Zhao, S.P. Yang, N.N. Ding, et al., Dalton Trans. 45 (2016) 5092–5100.
[141] H.T. Zhang, J.W. Zhang, G. Huang, et al., Chem. Commun. 50 (2014) 12069–12072.
[142] H.L. Tan, G.E. Tang, Z.X. Wang, et al., Anal. Chim. Acta 940 (2016) 136–142.
[143] R. Mejia-Ariza, J. Rosselli, C. Breukers, et al., Chem. -Eur. J. 23 (2017) 4180–4186.
[144] R.Y. Xu, Y.F. Wang, X.P. Duan, et al., J. Am. Chem. Soc. 138 (2016) 2158–2161.
[145] Y.H. Hu, H.J. Cheng, X.Z. Zhao, et al., ACS Nano 11 (2017) 5558–5566.
[146] Y. Lu, B. Yan, J.L. Liu, Chem. Commun. 50 (2014) 9969–9972.
[147] Y. Zhou, H.H. Chen, B. Yan, J. Mater. Chem. A 2 (2014) 13691–13697.
[148] J. Zhao, Y.N. Wang, W.W. Dong, et al., Inorg. Chem. 55 (2016) 3265–3271.
[149] B. Wang, Q. Yang, C. Guo, et al., ACS Appl. Mater. Interfaces 9 (2017) 10286–10295.
[150] D. Zhao, J. Zhang, D. Yue, et al., Chem. Commun. 52 (2016) 8259–8262.
[151] J.W. Zhang, H.T. Zhang, Z.Y. Du, et al., Chem. Commun. 50 (2014) 1092–1094.
[152] X.L. Yang, C.D. Wu, Inorg. Chem. 53 (2014) 4797–4799.
[153] M. Zhao, C.D. Wu, ChemCatChem 9 (2017) 1192–1196.
[154] C.D. Wu, M. Zhao, Adv. Mater. 29 (2017) 1605446.
[155] M.T. Zhao, Y.X. Wang, Q.L. Ma, et al., Adv. Mater. 27 (2015) 7372–7378.
[156] Y.K. Park, S.B. Choi, H. Kim, et al., Angew. Chem. Int. Ed. 46 (2007) 8230–8233.
[157] Y. Chen, V. Lykourinou, C. Vetromile, et al., J. Am. Chem. Soc. 134 (2012) 13188–13191.
[158] X.L. Wu, J. Ge, C. Yang, M. Hou, Z. Liu, Chem. Commun. 51 (2015) 13408–13411.
[159] X. Zhang, J.Y. Chen, X. Pei, et al., ACS Appl. Mater. Interfaces 9 (2017) 25171–25183.
[160] J.Y. Chen, X. Zhang, C. Huang, et al., J. Biomed. Mater. Res. A 105 (2017) 834–846.
[161] R. Abazari, A.R. Mahjoub, S. Molaie, et al., Ultrason. Sonochem. 43 (2018) 248–261.